

## COMPARISON WELDING PROCESS OF ROBOTIC GMAW ON THE FIRST PASS OF HIGH THICK ALUMINUM 6061

Milad Bahrami <sup>1</sup>, Michel Guillot <sup>2</sup>

<sup>1,2</sup>PI2/REGAL Research Team, Department of Mechanical Engineering, Laval University,  
Quebec, G1V 0A6, Canada  
e-mail: milad.bahrami.1@ulaval.ca, michel.guillot@gmc.ulaval.ca

**ABSTRACT:** In this study, the comparison of the first pass of the V groove bevel joint with 45 degree angle, root pass 2 mm and different root gap has been compared for automatic robotic gas metal arc welding (GMAW) of Aluminum 6061-T6 and optimized welding parameters such as voltage, wire feed speed, travel speed and distance of the gun to weld for the best weld of 6.35 mm, 12.7 mm, 19.05 mm and 25.4 mm were found. Taguchi technique based Orthogonal Array is used for Design of Experiments (DOE) and artificial neural network (ANN) modeling is utilized to predict the penetration, distortion and quality of the weld, as well as ultimate tensile strength (UTS) has been measured for 6.35 mm thickness. Finally, the ideal range of process parameters such as voltage, wire feed speed, distance between nozzle to work piece and travel speed have been identified.

**KEYWORDS:** Distortion, Gas Metal Arc Welding, Neural modeling, Penetration, Taguchi method, Welding parameters

### 1 INTRODUCTION

Aluminum is the most many metallic element in Earth's crust and the most widely used nonferrous metal.[1] AA6061 is a most precipitation-hardened aluminum alloy, containing magnesium and silicon as its major alloying elements. [2] It is commonly available in pre-tempered grades such as 6061-O (annealed), tempered grades such as 6061-T6 (solutionized and artificially aged) and 6061-T651 (solutionized, stress-relieved, stretched and artificially aged). [3] In previous searches, many welding methods have been used for the joining of aluminum alloys including gas metal arc welding (GMAW) [4-11], gas tungsten arc welding (GTAW) [12-14], friction stir welding (FSW) [15-18], laser beam welding [19-21], resistant spot welding [22], plasma-MIG welding [23]. Gas Metal Arc Welding (GMAW) process is one of the most widely used methods because it suits a wide range of applications. In the welding GMAW process, the weld quality depends on the joint preparation, electrode type, shielding gas, amperage

and voltage settings. [24] The distortion can extensively weaken the performance and consistency of the welded assembly. [25] and welding parameters such as current, voltage, wire feed speed and travel speed play a significant role in controlling them and leading to a good weld and to get a good quality weld and subsequently increase the productivity of the process, it is therefore, necessary to control the input welding parameters. [26] During welding residual stresses in structures are produced due to non-uniform thermal expansion and contraction of materials due to rapid, localized heating and non-linear temperature distributions. [27] These stresses are undesirable in welded components as they result in fatigue failure, stress corrosion cracking and impair the buckling strength of components. [28].

In the present work, an experimental study was conducted to compare and find the optimized welding parameters for first pass of the thick and thin butt weld joint to have minimum distortion and zero lack of penetration. Experiments were performed by varying process parameters such as voltage(V), wire feed speed (WFS), travel speed (TS), distance between weld and nozzle (DISW) with zero Gun Angle. Taguchi method was used to design the experiments. Penetration, Distortion and Quality of the weld have been measured for all samples and UTS has been measured for 6.35 mm thickness. The feedback of Voltage and Current from the welding machine has been measured to calculate the heat. After an artificial neural network (ANN) is created to predict and optimize welding parameters on penetration and distortion. Afterward, confirmation tests have been made to confirm the estimations of ANN models.

## 2 EXPERIMENTAL PROCEDURE

### 2.1 Material and equipment

**Material Properties and Consumable:** The base metal is 6061-T6 aluminum and the wire is 5356 with 1.2 mm diameter. Table 1 shows the material properties of the aluminum 6061-T6, and table 2 shows the material properties of this wire. Ceramic backing strip has been used and argon was gas shield with a flow of 0.71 cubic meters per hour (m<sup>3</sup>/hr) (25 cfh).

*Table 1.* (a) Chemical composition of aluminum 6061-T6 (b) Mechanical properties of aluminum 6061-T6

Material	Chemical Composition (wt%)							
	Al	Mg	Mn	Cu	Fe	Si	Ti	Zn
<b>AA-6061-T6</b>	Bal.	0.83	0.07	0.19	0.19	0.55	Max 0.15	Max 0.25

(b)

Mechanical Properties							
Material	Ultimate Tensile Strength	Tensile Yield Strength	Hardness, Brinell	Hardness, Knoop	Hardness, Rackwell A	Hardness Rackwell B	Hardness, Vickers
AA-6061-T6	310 MPa	276 MPa	95	120	40	60	107

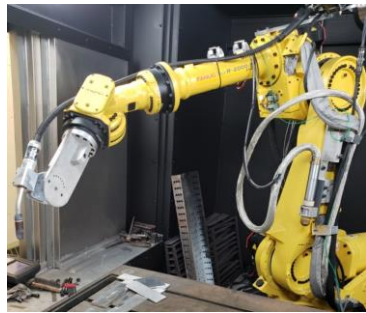
Table 2. (a) Chemical composition of wire 5356 (b) Physical Properties of wire 5356 (a)

Chemical Composition (wt%)							
Material	Al	Mg	Zn	Cu	Fe	Si	Other total
5356 Aluminum wire	92.9-95.3	4.5-5.5	0.1	0.10	0.4	0.25	0.15

(b)

Physical Properties								
Material	Solidus	Liquisus	Density	Post Anodize Color	Tensile Strength	Yield Strength	Elongation	Shear moduls (GPa)
5356 Aluminum wire	571 <sup>o</sup> C	635 <sup>o</sup> C	0.096	White	269 Mpa	131 Mpa	17%	26

**Robot and Welding Machine:** Fanuc R2000 robot and Miller Auto-Axcess 450 welding machine with pulsed arc welding technology are used to produce the welded samples. Figure 1 shows the process of working with a robot.



(a)



(b)

Figure 1. (a) Robot Fanuce R2000 (b) Miller Auto Axces 750

## 2.2 Joint preparation

In this paper, extruded flat bars of aluminum 6061 of size 245 mm×88 mm are supplied in the T6 condition. The butt welded V-Groove, 60 degree angle has been machined with 2 mm root face lengths, for joint preparation CNC Milling Machine has been used. Also, before any weld, all joints have been cleaned with acetone to make sure there is no dirt and dust on the joint. Different root gaps depending on thickness are set using calibrated shims, (Figure 2 Geometry of Joint).

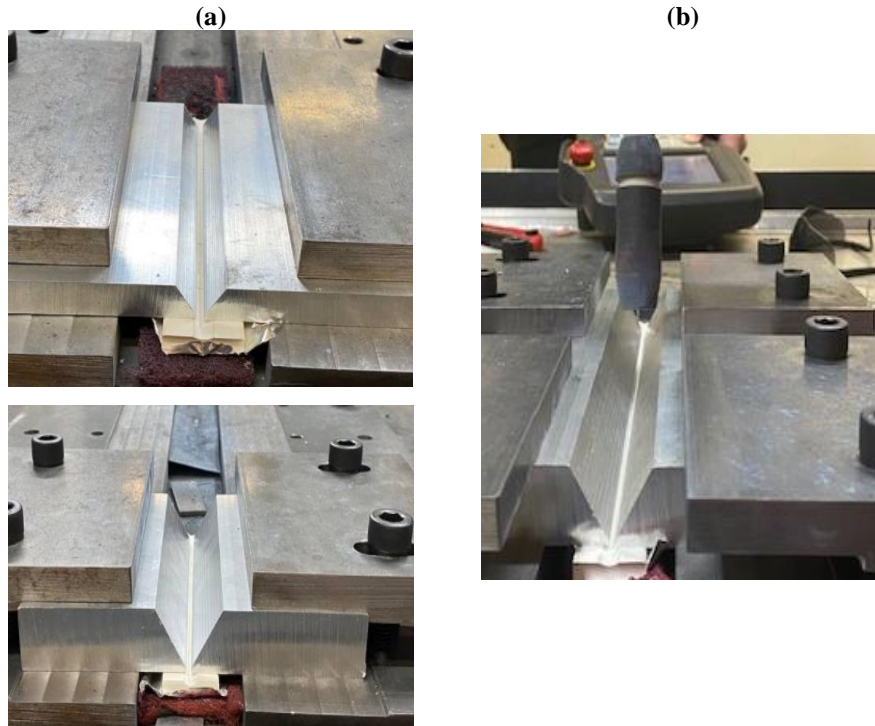


Figure 2. (a) Preparation of joint for 19 mm and 25 mm thick (b) Geometry of the joint with gun

### 2.3 Measurement/Quality evaluation

**Penetration (depth):** All samples have been cut, after that bend test has been performed by press machine to see penetration, and measure lack of penetration, (the lack of penetration on root has been measured using a digital caliper, and results indicated in mm, zero means has full penetration).

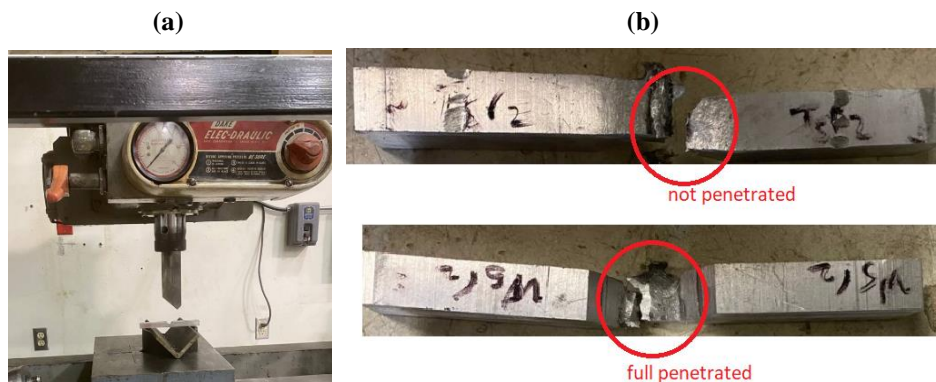


Figure 3. (a) Press machine for bend test (b) Root penetration

**Quality of the weld, stability:** In general, the stable weld means there is no surface defect like spatter, undercut, lack of fusion, etc. and the values are between -10(worst weld) to +10 (best weld) (Figure 4). Fluidity, by definition the shape of the penetration is called fluidity, the value of the fluidity is between -10(worst shape penetration) to +10(best shape penetration) the microstructure of the weld (Figure5).

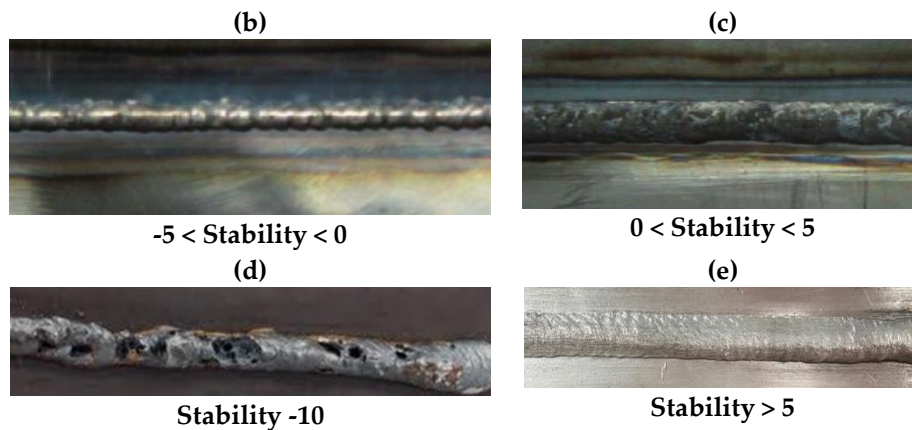


Figure 4. Stability of the weld

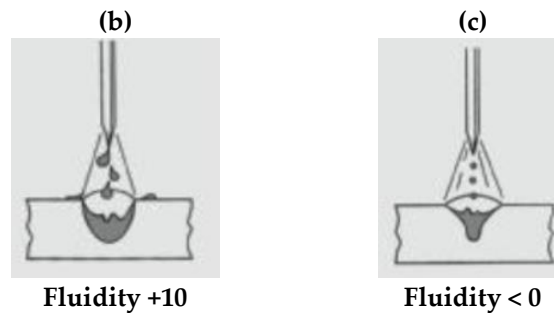


Figure 5. Fluidity of weld

**Distortion:** In this search distortion of the all plates has been measured by a based mounted digital indicator. Figure 6 shows schematic of distortion measurement and the equipment. On the top surface of the sample, 15 to 20 points measured (X-Y-Z). The data has been analyzed first by finding the best-fit plane, which is used as a reference plane.

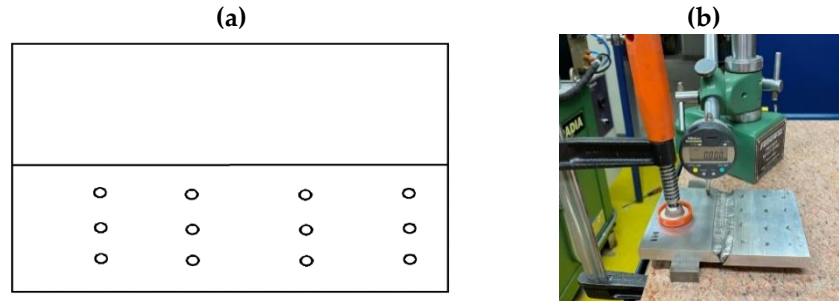


Figure 6. Distortion measurement (a) Position of 16 points on welded samples, (b) Current digital caliber equipment

## 2.4 Methodology

In this search, some steps have been followed. a) Find the best parameter of Accu-Pulsed process on weld bead. b) Prepare DOE by using results from step a for 6.35 mm and find optimized welding parameters for first pass c) By using results of step b, prepare DOE for first pass of the 12.7 mm and find optimized welding parameters d) By using results of step c, prepare DOE for first pass of the 19.05 mm and find optimized welding parameters e) By using results of step d, prepare DOE for first pass of the 25.4 mm and find optimized welding parameters.

### 2.4.1 Design of experiments

In this search, the design of experiments (DOEs) applies various orthogonal arrays accumulated and used to train an artificial neural network (ANN) model. First, preliminary tests were carried out for Accu-Pulsed mode on the extrusion of 25 mm thickness, and found the optimized weld parameters to have best penetration and maximum fluidity and stability. Table 3, shows the results of the preliminary test.

Table 3. Accu-Pulsed Process (a) Welding parameters for first preliminary tests

		Conditions set on the robot					Feedback from the robot	
		Travel speed	Wire speed	Voltage set	Distance nozzle to work	Torch forward angle	Voltage	Ampere
Samples	TS (mm/s)	WFS (mm/s)	(Volt)	Z (mm)	(deg)	V	A	
A	1	8	200	55	18	0	11.02	77.49
	2	8	200	55	17	0	14.71	136.69
	3	6	150	60	16	0	17.73	142.02
	4	7	200	50	15	0	15.97	154.09
	5	7	230	60	14	0	18.41	172.25
	6	6	200	55	15	0	16.92	148.62
	7	10	200	55	13	0	16.17	145.53
	8	6	200	65	13	0	16.41	171.84
	9	6	150	65	16	0	20.56	130.92
	10	8	200	65	17	0	21.57	171.06

**Table 3.** Accu-Pulsed Process (b) Results for first set of preliminary tests

	Penetration observations				Overall rating	Heat VxI	Visual aspects	
	Width A	Depth B	Height C	Section profile under the surface			Stability	Fluidity
Sample s	(mm)	(mm)	(mm)	(mm <sup>2</sup> )	(0 to 10)	Watt	(-10 to 10)	(0 to 10)
1	6.95	2.34	2.1	12.5664	1.5	854.13	3	3
2	9.5	2.4	4	28.2744	3	2011.3	8	5
3	8.7	1.3	4.2	28.2744	3	2517.3	8	5
4	9.8	2	4.2	32.3136	5	2460.8	7	3
5	12.1	3.96	4.9	37.1606	7	3171.1	8	4
6	11.58	3.2	4.4	37.6992	5	2514.6	7	3
7	9.1	2.7	3.7	22.6195	2	2353.2	6	3
8	10.7	2.4	4.5	37.6992	1	2819.8	6	4
9	9	1.25	3.78	28.2744	1	2691.7	4	3
10	9.6	2.4	3.5	28.2744	1	3689.7	4	3

#### 2.4.2 Artificial Neural Network (ANN) prediction model

In this study, an ANN was proposed to establish a relationship between output results and welding parameters. By using results from preliminary sets of the test (table 3), the ANN model had been trained. In this ANN model root-mean-square error (RMSE) and Maximum error have been calculated, RMSE is a frequently used measure of the differences between values (sample or population values) predicted by a model or an estimator and the values observed and Maximum error is the error is a measure of the difference between what the ANN predicts and the real label of data. Table 4 shows the best parameters which respect to have the best output results. Afterwards, based on acceptance levels of table 4, a final DOE (2C to 5C) was designed to explore more around the optimal region identified by the ANN model. This DOE has been made by using Taguchi L4 with input parameters such as voltage, wire feed speed, and travel speed. Table 5a shows the final DOE for experimental tests, and table 5b shows the results of these tests; in this set of tests, two more additional tests have been performed to find the better results (1C and 6C). For all samples, penetration included width, depth, and height, have been measured by a caliper. The best penetration for Accu-Pulse is width 13.7 mm, depth 4.2 mm and, height 5.3 mm (Figure 7).

**Table 4.** Best parameters from ANN

ACCU-Pulse	V	Travel speed	WFS	Distance nozzle to weld	Gun Angle
	55-60	5-7	230-260	14	0

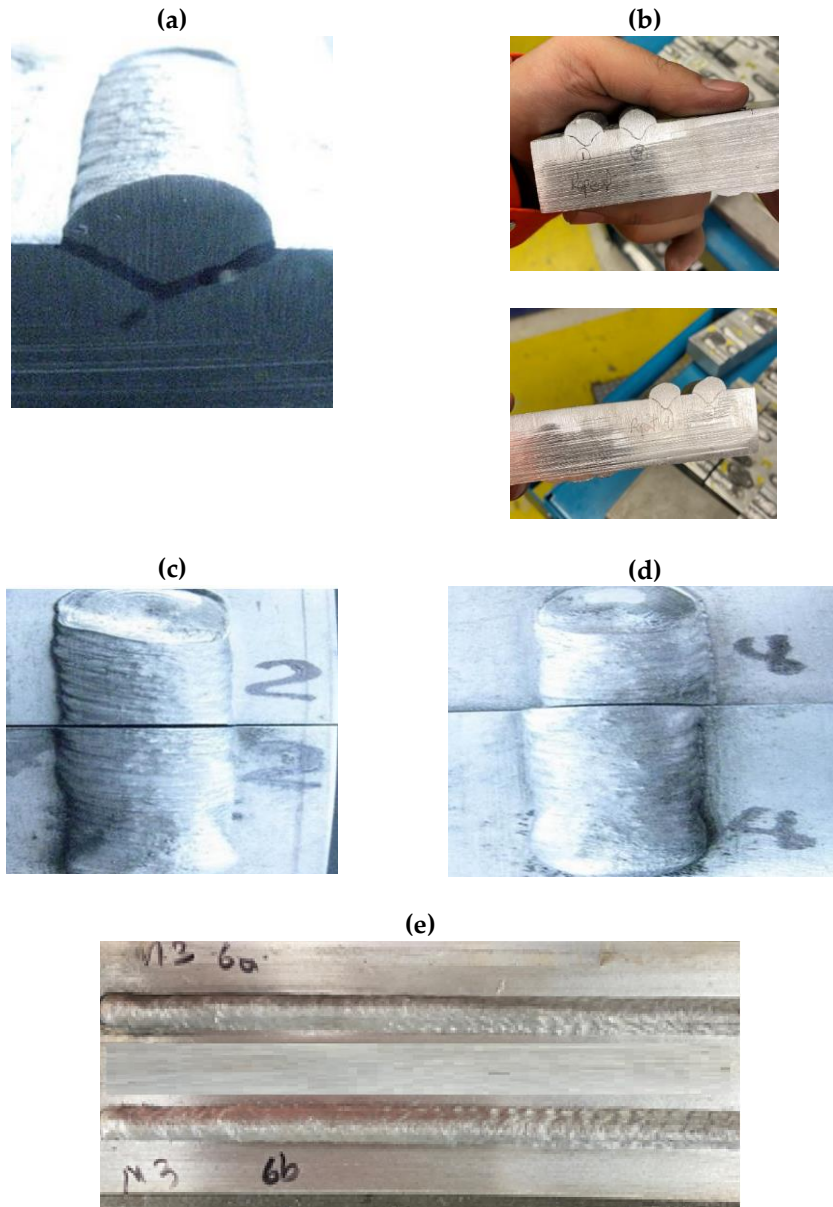


Figure 7. Weld samples for Accu-Pulse (a) penetration and fluidity of best sample (2C) (b) penetration and fluidity of confirmation sample (c) stability of the best sample (d) stability of confirmation sample (e) stability and overall rating of the confirmation sample.



*Table 5. Accu-Pulsed process*  
 (a) DOE of best parameters from ANN model (b) Results  
 (a)

		Conditions set on the robot					Feedback from the robot	
		Travel speed	Wire Feed Speed	Voltage set	Distance nozzle to work	Torch forward angle	Voltage	Ampere
C	Samples	TS (mm/s)	WFS (mm/s)	(Volt)	Z (mm)	(deg)	V	A
	1C	7	230	60	14	0	17.08	212.42
	2C	5	230	60	14	0	19.9	176.39
	3C	7	260	60	14	0	26.09	253.9
	4C	7	230	55	14	0	13.7	164.3
	5C	5	260	55	14	0	26.6	281.6
	6C	9	260	65	14	0	18.9	192

(b)

Samples	Penetration observations				Overall rating	Heat VxI	Visual aspects		
	Width A	Depth B	Height C	Section profile under the surface			Stability	Fluidity	Weld appearance
	(mm)	(mm)	(mm)	(mm <sup>2</sup> )	(0 to 10)	Watt	(-10 to 10)	(0 to 10)	
1C	11.6	3.26	4.8	37.16064	6.5	3628.13	8	4	
2C	13.7	4.2	5.3	52.0249	8.5	3510.16	8	4	Best with Accu-pulse
3C	12.4	3.9	4.4	42.00768	7	6624.25	8	4	
4C	11.8	4	4.6	37.16064	5	2250.91	5	3	
5C	not measurable	not measurable	not measurable	58.81075	0	7490.56	-3	2	unstable
6C	not measurable	not measurable	not measurable	58.81075	0	3628.80	-5	2	unstable

## 2.5 Optimization of the welding parameters for first pass

The first pass of the butt welded V-Groove 60 degree bevel angle has been performed for 6.35 mm, 12.7 mm, 19.05 mm and 25.4 mm thickness material.

**Thickness 6.35 mm:** Two preliminary tests were welded to find the range of the root gap, after that, L4 DOE has been designed with the travel speed, wire feed speed and root gap as welding parameters and input and used to train ANN model with penetration, stability and fluidity as an output (table 6). Optimized welding parameters have been found from the ANN model and confirmation test has been performed (Figure 8 shows the best example of penetration and distortion).

*Table 6. (a) Welding parameters for 6.35 mm thickness*

		Conditions set on the robot						Feedback from the robot	
		Travel speed	Wire Feed Speed	Root Gap	Voltage set	Distance nozzle to work	Torch forward angle	Voltage	Ampere
6.35 mm	Samples	TS (mm/s)	WFS (mm/s)	RG (mm)	(Volt)	Z (mm)	(deg)	V	A
	P11	5	240	0.762	55	13	0	24	180
	P12	7	225	3.75	55	13	0	23	170
	1	7	190	0.762	55	13	0	23	167
	2	7	195	1.4	55	13	0	24	170
	3	8	190	1.4	55	13	0	24	170
	4	8	195	0.762	55	13	0	25	175
	Best ANN	8	195	0.762	55	13	0	25	175
	Confirmation test	8	195	0.762	55	13	0	25	175

*Table 6. (b) Results*

Samples	Penetration observations				Heat VxI Watt	Visual aspects		
	Width	Depth	Section profile under the surface	Distortion		Stability	Fluidity	Overall Rating
	(mm)	(mm)	(mm <sup>2</sup> )	mm		(-10 to 10)	(0 to 10)	(0 to 10)
P11	23.43	6.3	54.28	0.24	4320	-3	5	2
P12	13.26	6.26	36.35	0.22	3910	-8	0	-4
1	12.64	6.38	30.69	0.2	3841	8	8	8
2	11.72	6.38	31.50	0.23	4080	7	8	7
3	10.56	6.38	26.68	0.24	4080	7	8	7
4	11.26	6.5	27.56	0.21	4375	9	9	9
Best ANN	11.5	6.6	27.56	0.2	4375	9	9	9
Confirmation test	11.5	6.6	27.56	0.2	4375	9	9	9

*Table 6. (c) UTS measurement*

Force	Area	UTS
KN	mm <sup>2</sup>	MPa
16857	40.32	206



Figure 8. (a) Best sample of the 6.35 mm thickness for penetration (b) Schematic of the Force Measurement (c) Final sample after UTS measurement.

**Thickness 12.7 mm:** By using the results from 6.35 mm thickness, two preliminary tests had been welded to find the range of the root gap and best travel speed. Afterward, an L4-DOE (table 7) was designed with wire feed speed, root gap and voltage as an input, and an ANN was proposed to establish a relationship between output results and welding parameters.

Table 7. (a) Welding parameters for 12.7 mm thickness

		Conditions set on the robot						Feedback from the robot	
		Travel speed	Wire Feed Speed	Root Gap	Voltage set	Distance nozzle to work	Torch forward angle	Voltage	Ampere
12.7 mm	Samples	TS (mm/s)	WFS (mm/s)	RG (mm)	(Volt)	Z (mm)	(deg)	V	A
	P11	7.5	195	1.4	55	10	0	20	185
	P12	6.5	195	2.1	58	12	0	21	187
	1	6	200	1.8	60	9	0	24	221
	2	6	200	2.1	62	9	0	25	200
	3	6	205	1.8	62	9	0	25	201
	4	6	205	2.1	60	9	0	25	204
	Best ANN	6	205	1.8	62	9	0	25	201
	Confirmation test 1	6	205	1.8	62	9	0	25	204
	Confirmation test 2	6	205	1.8	62	9	0	24.70	206

Table 7. (b) Results

Samples	Penetration observations				Heat VxI Watt	Visual aspects		
	Width (mm)	Depth (mm)	Section profile under the surface (mm <sup>2</sup> )	Distortion mm		Stability (-10 to 10)	Fluidity (0 to 10)	Weld appearance
P11	10.82	6.45	29.40	0.05	3700	6	6	6
P12	11.56	6.1	33.92	0.048	3927	7	6	6
1	13.97	6.35	37.92	0.06	5304	8	8	9
2	13.40	6.4	37.92	0.058	5000	7	7	7
3	13.73	6.6	38.64	0.05	5025	9	9	9
4	14.31	6.6	38.64	0.059	5100	8	8	8
Best ANN	14.5	6.6	3864	0.05	5025	9	9	9
Confirmation test	14.5	6.6	3864	0.05	5025	9	9	9

By using results from preliminary tests and DOE, the ANN model has been trained and outputs are as same as those of the 6.35 mm thickness. Optimized parameters have been found from the ANN model and two confirmation tests have been performed (Figure 9 shows the best samples of the 12.7 mm thickness).

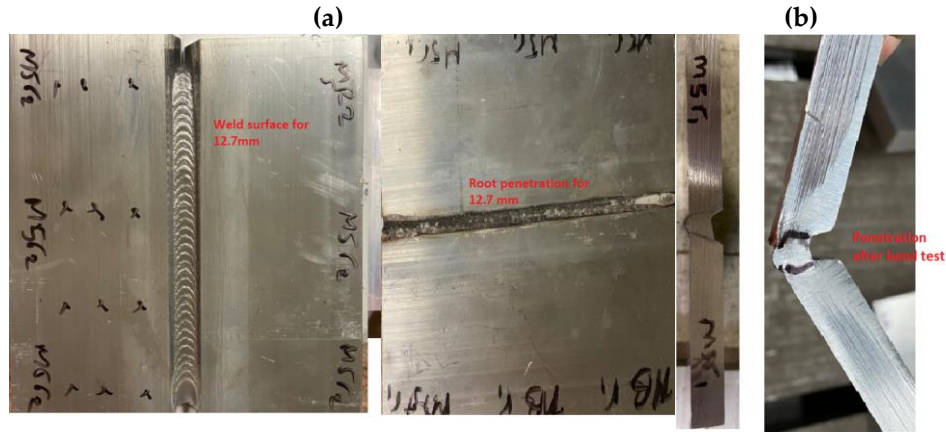


Figure 9. Best sample of the 12.7 mm thickness (a) penetration (b) Quality of weld

**Thickness 19.05:** By using the results from 12.7 mm thickness and travel speed of 6 mm/s the best distance of the weld has been found by two preliminary tests. Afterward, L4 DOE (table 8) has been designed with wire feed speed, voltage and root gap as input parameters and ANN model has been trained with same output parameters. Optimized parameters have been found from the ANN model and two confirmation tests have been performed (Figure 10 shows the confirmation test for 19.05 mm thickness).

Table 8. (a) Welding parameters for 19.05 mm thickness

		Conditions set on the robot						Feedback from the robot	
		Travel speed	Wire Feed Speed	Root Gap	Voltage set	Distance nozzle to work	Torch forward angle	Voltage	Ampere
19.05 mm	Samples	TS (mm/s)	WFS (mm/s)	RG (mm)	(Volt)	Z (mm)	(deg)	V	A
	P11	6	205	1.7	62	5	0	25.64	212
	P12	6	205	1.9	62	5	0	25.45	199
	1	6	205	1.9	62	3	0	26	200
	2	6	205	2.2	66	3	0	26.5	210
	3	6	208	1.9	66	3	0	27	208
	4	6	208	2.2	62	3	0	24	205
	Best ANN	6	208	2.2	66	3	0	23.8	265
	Confirmation test 1	6	208	2.2	66	3	0	23.8	266
	Confirmation test 2	6	208	2.2	66	3	0	23.8	266

Table 8. (b) Results

Samples	Penetration observations				Heat VxI Watt	Visual aspects		
	Width	Depth	Section profile under the surface	Distortion		Stability	Fluidity	Weld appearance
	(mm)	(mm)	(mm <sup>2</sup> )	mm		(-10 to 10)	(0 to 10)	
P11	14.5	6.7	38.64	0.04	5435	5	8	6
P12	14.11	6.5	38.64	0.025	5064	7	8	7
1	14.15	6.6	38.64	0.03	5200	7	8	7
2	13.5	6.8	38.64	0.045	5565	8	8	8
3	14.5	6.8	39.20	0.05	5616	8	9	8
4	13.8	6.5	39.20	0.04	4920	9	9	9
Best ANN	15.5	6.5	39.20	0.06	6307	9	9	9
Confirmation test	15.5	6.5	39.20	0.06	6307	9	9	9

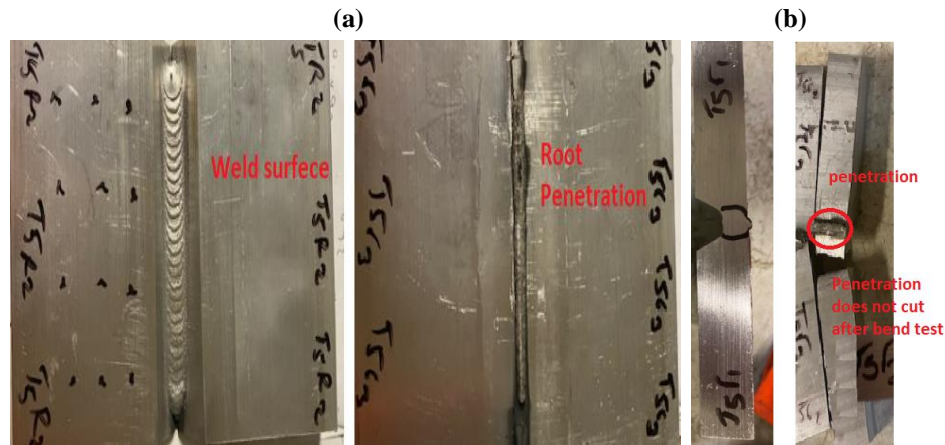


Figure 10. Best sample of the 19.05 mm thickness (a) penetration (b) Quality of weld

**Thickness 25.4 mm:** By using results from 12.7 mm and 19.07 mm thickness, two preliminary tests have been welded, and in the results have been found not fully penetrated and the problem looks like carbon penetration (Figure 11a). So, in order to have better penetration more literature review has been done, and we have decided to increase gas flow, so L4 DOE (table 9) has been performed by using gas flow, root gap and voltage as input. After that, the ANN model has been carried out with the same output results. Optimized parameters have been found and two confirmation tests have been performed. (Figure 11b shows the confirmation tests for 25.4 mm thickness)

Table 9. (a) Welding parameters for 25.4 mm thickness

	Samples	Conditions set on the robot							Feedback from the robot	
		Travel speed	Wire Feed Speed	Gas Flow	Root Gap	Voltage set	Distance nozzle to work	Torch forward angle	Voltage	Ampere
		TS (mm/s)	WFS (mm/s)	GF CFH	RG mm	(Volt)	Z (mm)	(deg)	V	A
25.4 mm	P11	6	205	25	1.8	62	3	0	24.7	212
	P12	6	205	25	2	66	3	0	25	215
	P13	6	210	40	2	66	3	0	26.10	234
	1	6	210	25	2	66	3	0	27.5	250
	2	6	210	25	2.2	70	3	0	29	242
	3	6	210	40	2	70	3	0	26.4	234
	4	6	210	40	2.2	66	3	0	26.10	234
	Best ANN	6	210	40	2	70	3	0	26.4	234
	Confirmation test 1	6	210	40	2	70	3	0	26.3	234
	Confirmation test 2	6	210	40	2	70	3	0	26.3	234

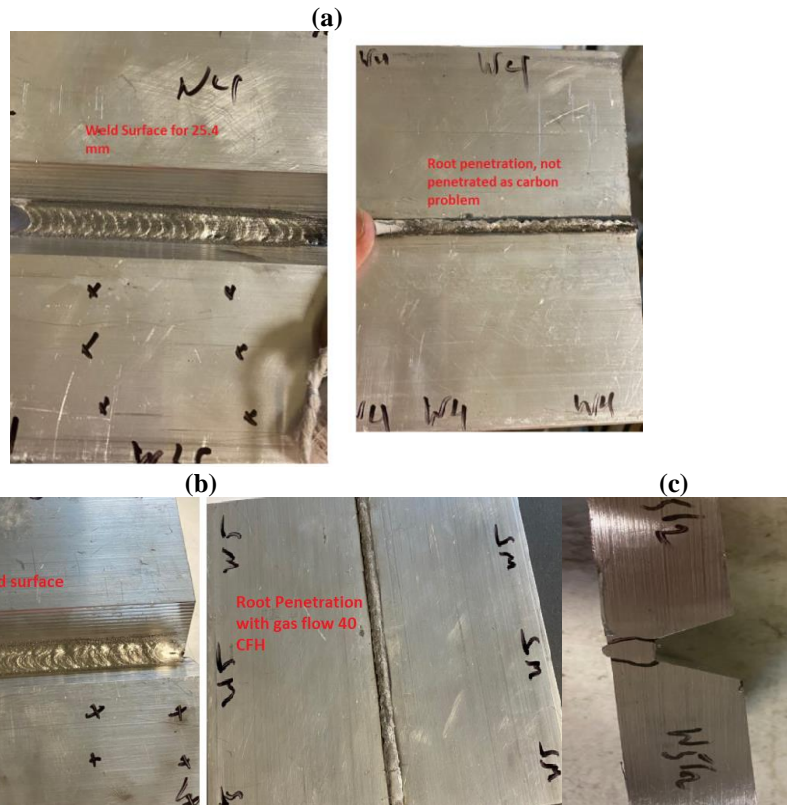


Figure 11. (a) Sample with 25 CFH gas flow (b) Best sample of the 25.4 mm thickness penetration with 40 CFH (c) Quality of weld

Table 9. (b) Results

Samples	Penetration observations				Heat VxI Watt	Visual aspects		
	Width	Depth	Section profile under the surface	Distortion		Stability	Fluidity	Weld appearance
	(mm)	(mm)	(mm <sup>2</sup> )	mm		(-10 to 10)	(0 to 10)	
P11	14.5	6.5	39.20	0.03	5236	4	2	No penetration
P12	15.5	6.4	39.20	0.03	5375	4	1	No penetration
P13	15.8	6.8	39.58	0.035	6107	5	5	
1	14.1	7	39.58	0.038	6875	1	2	
2	16	7	39.58	0.041	7018	4	4	
3	15.4	6.8	39.58	0.03	6107	7	8	
4	15.5	6.5	39.58	0.03	6177	7	8	
Best ANN	15.4	6.8	39.58	0.03	6107	8	8	
Confirmation test	15.4	6.8	39.58	0.03	6107	8	8	

### 3 RESULTS AND DISCUSSION

#### 3.1 Penetration

For all samples, penetration included width, depth, and height, have been measured by a caliper. The best penetration for all thickness has been shown.

#### 3.2 Stability, fluidity and distortion

As explained in part 2.2, the stability and fluidity of the weld has been checked for all samples visually. As well as distortion has been measured by equipment digital caliper.

#### 3.3 Voltage and current feedback from the welding machine

**Feed back from Robot and Calculation Heat:** In the program, input voltage is depends on the machine, robot and program, but the exact voltage and current have been measured and are feedback from miller Machine, and heat is calculated the multiple of the feedback, current and voltage from welding machine.

### 4 CONCLUSIONS

Parameter optimization based on experimental samples and ANN models has been presented in this paper. In this study, Gas Metal Arc Welding was used on the bead geometry of Aluminum 6061 with Accu-Pulse mode and four different welding processes such as 6.35, 12.7, 19.05 and 25.4 mm bevel angle with 60 degree and 2 mm root face. The following conclusions were found noteworthy on the basis of this investigative work:

- The best parameters for welding according to this search have been found and show in table 10.



- The optimum process parameters recommended by the study are:

*Table 10. Optimum process parameters*

Welding Parameters	6.35 mm	12.7 mm	19.05 mm	25.4 mm
WFS (mm/s)	195	205	208	210
TS (mm/s)	8	6	6	6
V (feedback v)	25	25	23.8	23.63
DISW (mm)	13	9	3	3
GA (degree)	0	0	0	0
Gas Flow (CFH)	25	25	25	40
Root Gap	0.762	1.8	2.2	2
Heat (Watt)	4337	5025	6307	6107

- WFS, TS and V were the input parameters that showed a more significant effect on the weld penetration characteristics.
- For high thick material like 25.4, with gas flow 25 CFH, there is no full penetration and has carbon problem, but increasing 65% gas flow, full penetration has been reached.

### Author Contributions:

**Funding:** This research has been supported by funds of PI<sup>2</sup> Team.

**Conflicts of Interest:** The authors declare no conflict of interest.

### REFERENCES

- [1] ASM Handbook, Volume 2: Properties and Selection: Nonferrous Alloys and Special-Purpose Materials ASM Handbook Committee, p 102 DOI: 10.1361/asmhba0001060.
- [2] Robert E. Sanders, Jr. (2001). "Technology Innovation in Aluminum Products". JOM. 53 (2): 21–25. Bibcode:2001JOM....53b..21S. doi:10.1007/s11837-001-0115-7. S2CID 111170376
- [3] H. Hekmatjou, H. Naffakh-Moosavy, Hot cracking in pulsed Nd:YAG laser welding of AA5456, Laser Technol., 103 (2018), pp. 22-32, 10.1016/j.optlastec.2018.01.020.
- [4] PraveenMath et al, Optimization of MIG welding process parameters to predict maximum yield strength in AISI 1040, International Journal of Mechanical Engineering and Robotics Research, 1 (3) (2012), pp. 203-213.
- [5] K.G. Chandiramani, Testing and Grading of Metal Arc Welding, Int. J. Prod. Res., 6 (4) (2007), pp. 281-290, 10.1080/00207546708929787.
- [6] I. Pires, L. Quintino, R.M. Miranda, Analysis of the influence of shielding gas mixtures on the gas metal arc welding metal transfer modes and fume formation rate, Materials & Design Volume 28, Issue 5, 2007, Pages 1623-1631.
- [7] KaiyuanWu et al, Metal transfer of aluminum alloy double-wire pulsed GMAW with a median waveform, Journal of Materials Processing Technology Volume 286, December 2020, 116761
- [8] B. Yu, Y. Chen Driving rhythm method for driving comfort analysis on rural highways Promet Zagreb, 29 (4) (2017), pp. 371-379.
- [9] K. Weman and G. Lindén (eds). MIG Welding Guide, Woodhead Publishing 2006.
- [10] G. Singh, S. Kumar, A. Singh Influence of current on microstructure and hardness of butt welding aluminium AA6082 using GTAW process, Int. J. Res. Mech. Eng. Technol., 3 (2013), pp. 143-146.

- [11] P.T. Trivedi, A.P. Bhabhor, A Review on Effect of Process Parameters on Weld Bead for GTAW, *Int. J. Eng. Manage. Res.*, 4 (2014), pp. 22-26.
- [12] L.H. Shah, N. Azhani, A. Razak, A. Juliawati, M. Ishak, Investigation on the mechanical properties of TIG Welded AA6061 alloy weldments using different aluminium fillers, *GSTF J. Eng. Technol.*, 2 (2013).
- [13] M.A. Abdulstaar, K.J. Al-fadhlah, L. Wagner Microstructural variation through weld thickness and mechanical properties of peened friction stir welded 6061 aluminum alloy joints *Mater. Charact.*, 126 (2017), pp. 64-73.
- [14] M Abu-okail, I. Sabry, A. Abu-okail, W.M. Shewakh, Effect of changing heat treatment conditions on microstructural and mechanical properties of friction stir welded sheets of AA2024 with interlayer strip width AA7075, *J. Fail. Anal. Prev.*, 20 (2020), pp. 701-722.
- [15] Chandran , R. Chandran, S. Kumar, V. Santhanam Submerged friction stir welding of 6061-T6 aluminium alloy under different water heads, *Mater. Res.*, 21 (2018), p. 6.
- [16] M. Dehghani, A. Amadeh, S., A.A.A. Mousavi Investigations on the effects of friction stir welding parameters on intermetallic and defect formation in joining aluminum alloy to mild steel *Mater. Des.*, 49 (2013), pp. 433-441.
- [17] H.A. Derazkola, F. Khodabakhshi, Underwater submerged dissimilar friction-stir welding of AA5083 aluminum alloy and A441 AISI steel *Int. J. Adv. Manuf. Technol.*, 102 (9-12) (2019), pp. 4383-4395.
- [18] N. Ethiraj, T. Sivabalan, S. Meikeerthy, K.L.V.R. Kumar, G. Chaithanya, G.P.K. Reddy, Comparative study on conventional and underwater friction stir welding of copper plates comparative study on conventional and underwater friction stir welding of copper plates, *International Conference on Materials, Manufacturing and Machining* (2019).
- [19] W. Guo, Z. Wan, Q. Jia, L. Ma, H. Zhang, C. Tan, P. Peng Laser weldability of TWIP980 with DP980/B1500HS/QP980 steels: Microstructure and mechanical properties *Opt. Laser Technol.*, 124 (2020), p. 105961.
- [20] K.I. Yaakob, M. Ishak, M.M. Quazi, M.N.M. Salleh Optimizing the pulse wave mode low power fibre laser welding parameters of 22Mnb5 boron steel using response surface methodology *Meas. J. Int. Meas. Confed.*, 135 (2019), pp. 452-466.
- [21] D.C. Saha, E. Biro, A.P. Gerlich, N.Y. Zhou, Fusion zone microstructure evolution of fiber laser welded press-hardened steels *Scr. Mater.*, 121 (2016), pp. 18-22.
- [22] J. Valera, V. Miguel, A. Martínez, J. Naranjo, M. Cañas, Optimization of electrical parameters in Resistance Spot Welding of dissimilar joints of micro-alloyed steels TRIP sheets *Procedia Manufacturing*, 13 (2017), pp. 291-298.
- [23] Tao Yang et al, Arcs interaction mechanism in Plasma-MIG hybrid welding of 2219 aluminium alloy, *Journal of Manufacturing Processes Volume 56, Part A, August 2020, Pages 635-642.*
- [24] Fuyun Liu et al, Improvement of penetration ability of heat source for 316 stainless steel welds produced by alternating magnetic field assisted laser-MIG hybrid welding, *Journal of Materials Processing Technology Volume 299, January 2022, 117329.*
- [25] Venkatkumar d, Ravindran d, Selvakumar G. Finite element analysis of heat input effect on temperature, residual stresses and distortion in butt welded plates [J]. *Materials Today Proceedings*, 2018, 5: 8328–8337.
- [26] Amirreza KHOSHROYAN et al, Effects of welding parameters and welding sequence on residual stress and distortion in Al6061-T6 aluminum alloy for T-shaped welded joint, *Trans. Nonferrous Met. Soc. China* 30(2020) 76–89.
- [27] R. Schasse, Th. Kannengiesser, A. Kromm, T. Mente, Residual stresses in repair welds of high-strength low-alloy steels, *Weld World*, 59 (2015), pp. 757-765.
- [28] R.K. Hemmesi, M. Farajian, D. Siegele, Numerical and experimental description of the welding residual stress field in tubular joints for fatigue assessment *Weld World*, 60 (2016), pp. 741-748.